Available online at www.sciencedirect.com
SCIENCE DIRECT
Journal of Organometallic Chemistry 691 (2006) 3919–3930
Journal of Organometallic Chemistry
www.elsevier.com/locate/jorganchem

Tin(IV) complexes obtained by reacting 2-benzoylpyridine-derived thiosemicarbazones with $SnCl_4$ and Ph_2SnCl_2

Anayive Pérez-Rebolledo [a], Geraldo M. de Lima [a], Nivaldo L. Speziali [b], Oscar E. Piro [c], Eduardo E. Castellano [d], José D. Ardisson [e], Heloisa Beraldo [a,*]

[a] Departamento de Química, Universidade Federal de Minas Gerais, 31270-901, Belo Horizonte, MG, Brazil
[b] Departamento de Física, Universidade Federal de Minas Gerais, 31270-901, Belo Horizonte, MG, Brazil
[c] Departamento de Física, Facultad de Ciencias Exactas, Universidad Nacional de La Plata and Instituto IFLP(CONICET), C.C. 67, 1900 La Plata, Argentina
[d] Instituto de Física de São Carlos, Universidade de São Paulo, C.P. 369, 13560-970 São Carlos (SP), Brazil
[e] Centro de Desenvolvimento da Tecnologia Nuclear, CDTN, 31270-901, Belo Horizonte, MG, Brazil

Received 23 February 2006; received in revised form 23 May 2006; accepted 24 May 2006
Available online 7 June 2006

Abstract

Reaction of 2-benzoylpyridine thiosemicarbazone (H2Bz4DH, HL1) and its N(4)-methyl (H2Bz4Me, HL2) and N(4)-phenyl (H2Bz4Ph, HL3) derivatives with $SnCl_4$ and diphenyltin dichloride (Ph_2SnCl_2) gave $[Sn(L1)Cl_3]$ (**1**), $[Sn(L1)PhCl_2]$ (**2**), $[Sn(L2)Cl_3]$ (**3**), $[H_2L2]_2^+[Ph_2SnCl_4]^{2-}$ (**4**) $[Sn(L3)PhCl_2]$ (**5**) and $[Sn(L3)Ph_2Cl]$ (**6**). Infrared and ^1H, ^{13}C and ^{119}Sn NMR spectra of **1**–**3**, **5** and **6** are compatible with the presence of an anionic ligand attached to the metal through the N_{py}–N–S chelating system and formation of hexacoordinated tin complexes. The crystal structures of **1**–**3**, **5** and **6** show that the geometry around the metal is a distorted octahedron formed by the thiosemicarbazone and either chlorides or chlorides and phenyl groups. The crystal structure of **4** reveals the presence of $[H_2L2]_2^+$ and *trans* $[Ph_2SnCl_4]^{2-}$.

Keywords: 2-Benzoylpyridine thiosemicarbazones; Tin(IV) complexes; Phenyltin(IV); Diphenyltin(IV); Crystal structures

1. Introduction

Thiosemicarbazones and their metal complexes present a wide range of pharmacological applications. Their antitumoral as well as their antifungal and antibacterial activities have been extensively reported in the literature [1]. Tin complexes are also known for their biological interest as antitumorals, antimicrobials and biocides [2a,2b,2c]. The therapeutic potential of some organotin compounds has been studied [2d,2e,2f].

With this in mind some groups investigated whether thiosemicarbazones and tin could act synergistically. It was found that dimethyltin complexes of 2-formylpyridine and 2-acetylpyridine-derived thiosemicarbazone strongly inhibit the growth of Friend leukemia cells (FLC) [3]. Additionally, the ability of $[Sn(L)R_2]$ (R = methyl, *n*-butyl, phenyl) complexes of pyridoxal thiosemicarbazone to inhibit FLC proliferation has been evaluated, and the *n*-butyl- and phenyl-tin derivatives showed the lowest thresholds for inhibition [4].

Previously, some of us prepared tin(IV) complexes of N(4)-phenyl-2-benzoylpyridine thiosemicarbazone (H2Bz-4Ph) and studied their antifungal properties [5]. We also demonstrated the cytotoxic activity of *n*-butyltin complexes of H2Bz4Ph against three human tumor cell lines. The di-*n*-butyl compound proved to be particularly effective [6].

Considering the necessity for further research on bioactive tin compounds, in the present work we carried out reactions between 2-benzoylpyridine thiosemicarbazone

* Corresponding author. Tel.: +55 31 3499 5740; fax: +55 31 3499 5700.
E-mail address: hberaldo@ufmg.br (H. Beraldo).

0022-328X/$ - see front matter © 2006 Elsevier B.V. All rights reserved.
doi:10.1016/j.jorganchem.2006.05.046

(H2Bz4DH, hereafter named HL1) as well as its N(4)-methyl (H2Bz4Me, HL2) and N(4)-phenyl (H2Bz4Ph, HL3) (Fig. 1) derivatives with $SnCl_4$ and Ph_2SnCl_2 in order to obtain complexes with potential applications as cytotoxic or antimicrobial agents. The pharmacological profiles of the studied compounds are presently under investigation.

2. Experimental

2.1. Materials and measurements

Tin tetrachloride and diphenyltin dichloride were purchased from Sigma–Aldrich and used without further purification. All other chemicals and solvents were of analytical grade.

Partial elemental analyses were performed on a Perkin–Elmer CHN 2400 analyzer. Atomic absorption analyses were carried out with a Hitachi Z-8200 equipment. Infrared spectra were recorded on a Perkin–Elmer FT-IR Spectrum GX spectrometer using CsI pellets; an YSI model 31 conductivity bridge was employed for molar conductivity measurements; NMR spectra were obtained with a Bruker DRX-400 Avance (400 MHz) spectrometer using deuterated dimethylsulfoxide (DMSO-d_6). The ^1H and ^{13}C NMR chemical shifts in ppm are reported from internal tetramethylsilane (TMS) on the % scale. The ^{119}Sn NMR spectra were measured relative to $Sn(CH_3)_4$.

2.2. Crystal structure determination

Crystal data, data collection procedure, structure determination methods and refinement results for the six tin(IV) complexes are summarized in Tables 1–3.

In all six structures, the hydrogen atoms were positioned on stereo-chemical basis and refined either with the riding model (compounds **1**–**4**) or isotropically [**5** and **6**]. The methyl H-atoms positions of compound **4** were optimized by considering the CH_3 as a rigid group that was allowed to rotate around the N–CH_3 bond during the refinement.

2.3. Synthesis of [Sn(L1)Cl$_3$] (1), [Sn(L1)PhCl$_2$] (2), [Sn(L2)Cl$_3$] (3), [H$_2$L2]$_2$[Ph$_2$SnCl$_4$] (4), [Sn(L3)PhCl$_2$] (5) and [Sn(L3)Ph$_2$Cl] (6)

The 2-benzoylpyridine derived thiosemicarbazones were prepared as described in the literature [7,8]. The tin complexes were obtained by refluxing an ethanol solution of the desired ligand with $SnCl_4$ or Ph_2SnCl_2 in 1:1 ligand-to-metal molar ratio. Complexes **5** and **6** were obtained as two products of the same reaction. The solids were washed with ethanol followed by diethylether and then dried *in vacuo*. Crystals of the complexes were obtained by re-crystallization from ethanol and were stable in the air for several hours.

2.3.1. [Sn(L1)Cl$_3$] (1)

Yellow solid. M.p.: 246.2–246.8 °C. Anal. Calc. $C_{13}H_{11}N_4Cl_3SSn$ (480.39): C, 32.50; H, 2.31; N, 11.66; Sn, 24.41. Found: C, 33.85; H, 2.36; N, 11.27, Sn, 25.05%. Molar conductivity (1×10^{-3} mol L^{-1} DMF): 9.42 Ω^{-1} cm^2 mol^{-1}. IR (CsI pellets, cm^{-1}): 1543m ν(C=N), 715m ν(C—S), 657m ρ(py), 360m ν(M–N), 336m ν(M–S), 259m ν(M–Npy), 305m, 220w ν(M–Cl). The main signals in ^1H NMR (DMSO-d_6): δ (ppm) = 9.13 (1H, d, H(6)), 8.83 (2H, s, N(4)H), 8.40 (1H, t, H(4)), 8.08 (1H, dd, H(5)), 7.72–7.60 (1H, d, H(3)). The main signals in ^{13}C NMR (DMSO-d_6): δ (ppm) = 171.74 C8—S, 144.42 C6, 144.42 C4, 142.02 C2, 140.33 C7=N, 129.80 C9, 128.20 C5, 127.29 C3. ^{119}Sn NMR (DMSO): δ (ppm) = −471 (s).

2.3.2. [Sn(L1)PhCl$_2$] (2)

Yellow solid. M.p.: 264.8–265.3 °C. Anal. Calc. $C_{19}H_{16}N_4Cl_2SSn$ (522.01): C, 43.71; H, 3.09; N, 10.73;

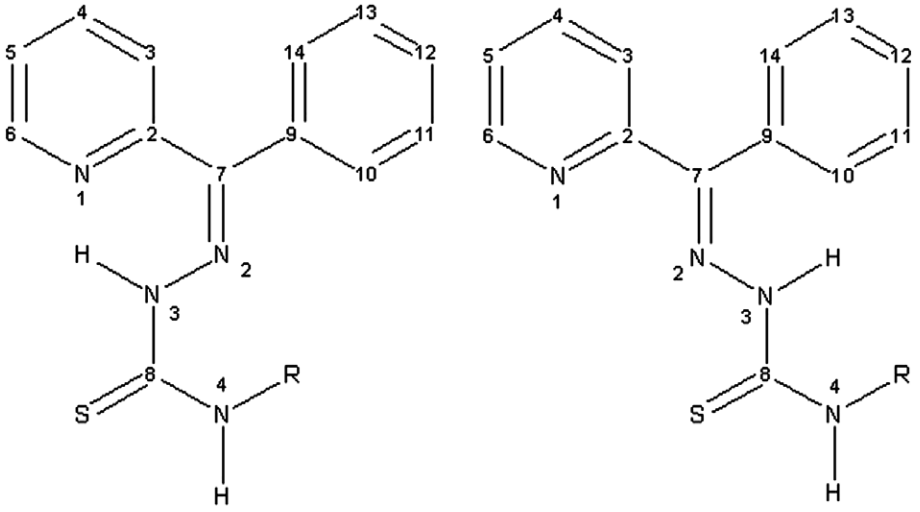

Fig. 1. Generic structure of 2-bezoylpyridine-derived thiosemicarbazones showing the *Z* (left) and *E* (right) configurational isomers. R = H (H2Bz4DH, HL1), methyl (H2Bz4Me, HL2) or phenyl (H2Bz4Ph, HL3).

Table 1
Crystal data, structure solution methods and refinement results for [Sn(L1)Cl_3] (**1**) and [Sn(L1)$PhCl_2$] (**2**) complexes

Compound	[Sn(L1)Cl_3]	[Sn(L1)$PhCl_2$]
Empirical formula	$C_{13}H_{11}N_4Cl_3SSn$	$C_{19}H_{16}N_4Cl_2SSn$
Formula weight	480.39	522.01
Temperature (K)	293(2)	293(2)
Crystal system	Monoclinic	Monoclinic
Space group	$P2_1/n$	Pn
Unit cell dimensions[a]		
a (Å)	8.305(4)	7.970(1)
b (Å)	12.485(3)	11.287(1)
c (Å)	17.200(5)	11.725(1)
β (°)	100.89(3)	96.382(5)
Volume (Å^3)	1751(1)	1048.2(2)
Z, density calc. (Mg m^{-3})	4, 1.822	2, 1.654
Absorption coefficient, μ (mm^{-1})	2.035	1.585
$F(000)$	936	516
Crystal size (mm)	$0.12 \times 0.12 \times 0.12$	$0.03 \times 0.04 \times 0.18$
Crystal color, shape	Yellow, prism	Yellow, needle
Diffractometer, scan	SIEMENS-P4;$2\theta - \omega$	KappaCCD/φ and ω
Rad., graph. Monoch.	Mo Kα, $\lambda = 0.71073$ Å	Mo Kα, $\lambda = 0.71073$ Å
θ Range for data coll. (°)	2.03–24.99	3.14–24.99
Index range, θ	$-6 \leqslant h \leqslant 9$	$-9 \leqslant h \leqslant 9$
	$-1 \leqslant k \leqslant 14$	$-13 \leqslant k \leqslant 13$
	$-20 \leqslant l \leqslant 20$	$-12 \leqslant l \leqslant 13$
Completeness	100% to $\theta = 24.99°$	99.6% to $\theta = 25.36°$
Absorption correction	Spherical [17]	Multi-scan [18]
Max. and min. transm.	0.8614 and 0.8618	0.835 and 0.766
Obs. refls. [$I > 2\sigma(I)$]	2663	3030
Data collection	XSCANS [19]	COLLECT [20]
Data red. and correct.[b] and struct. solute[c] and refinement[d] programs	XSCANS [19]	DENZO and SCALEPACK [21]
	SHELXS-97 [22]	SHELXS-97 [22]
	SHELXL-97 [23]	SHELXL-97 [23]
Refinement method	Full-matrix least-squares on F^2	Full-matrix least-squares on F^2
Goodness-of-fit on F^2	0.982	1.099
Reflections collected/unique [R_{int}]	6028/3079 (0.0352)	4765/3173 [0.0776]
Data/restraints/parameters	3079/0/199	3173/2/245
R_{obs}, R_{all}	0.0369, 0.0445	0.0658, 0.0677
wR_{2obs}, wR_{2all}	0.1127, 0.1227	0.1698, 0.1752
Larg. peak and hole (e Å^{-3})	0.733 and −1.004	2.08 and −1.50

[a] Least-squares refinement of the angular settings for 32 reflections in the $10.29° < \theta < 17.3°$ range for **1** and 4765 reflections in the $3.14° < \theta < 24.99°$ range for **2**.
[b] Corrections: Lorentz and polarization for **1** and **2**. Absorption correction was numerical for **1** and empirical for **2**.
[c] Neutral scattering factors and anomalous dispersion corrections.
[d] Structure solved by direct and Fourier methods. The final molecular model obtained by anisotropic full-matrix least-squares refinement of the non-hydrogen atoms.

Sn, 22.74. Found: C, 44.21; H, 2.90; N, 10.75; Sn, 23.71%. Molar conductivity (1×10^{-3} mol L^{-1} DMF): 6.07 Ω^{-1} cm^2 mol^{-1}. IR (CsI pellets, cm^{-1}): 1551m ν(C═N), 730m ν(C─S), 654m ρ(py), 265w ν(M–C), 360m ν(M–N), 319w ν(M–S), 242w ν(M–Npy), 210w ν(M–Cl). The main signals in ^{1}H NMR (DMSO-d_6): δ (ppm) = 8.29–8.23 (1H, m, H(6)), 8.45 (1H, s, N(4)H), 8.29–8.23 (1H, m, H(4)), 8.29–8.23 (1H, m, H(3)), 7.82 (1H, dd, H(5)). The main signals in ^{13}C NMR (DMSO-d_6): δ (ppm) = 172.65 C8─S, 144.08 C2, 143.71 C6, 143.25 C4, 142.99 C7═N, 131.01 C9, 127.10 C5, 126.36 C3; 139.66 C21, 135.28 C22 and C26, 130.29 C24, 128.84 C23 and C25. $^nJ(^{119}Sn^{13}C)$: 296.7 Hz $^1J(^{119}Sn^{13}C21)$, 82.1 Hz $^2J(^{119}Sn^{13}C22$, C26), 123.8 Hz $^3J(^{119}Sn^{13}C23$, C25), 24.4 Hz $^4J(^{119}Sn^{13}C24)$ and 27.6 Hz $^2J(^{119}Sn^{13}C6)$. ^{119}Sn NMR (DMSO): δ (ppm) = −374 (s).

2.3.3. [Sn(L2)Cl_3] (**3**)

Yellow solid. M.p.: 279.0–280.2 °C. Anal. Calc. $C_{14}H_{13}N_4Cl_3SSn$ (494.38): C, 34.01; H, 2.65; N, 11.33; Sn, 24.01. Found: C, 34.11; H, 2.59; N, 11.33; Sn, 24.39%. Molar conductivity (1×10^{-3} mol L^{-1} DMF): 8.96 Ω^{-1} cm^2 mol^{-1}. IR (CsI pellets, cm^{-1}): 1554s ν(C═N), 721m ν(C─S), 633w ρ(py), 353w ν(M–N), 338m ν(M–S), 249w ν(M–Npy), 308m, 210w ν(M–Cl). The main signals in ^{1}H NMR (DMSO-d_6): (δ, ppm) = 9.14 (1H, d, H(6)), 9.17 (2H, q, N(4)H), 8.44 (1H, t, H(4)), 8.11 (1H, dd, H(5)), 7.83 (1H, d, H(3)), 2.79 (1H, d, H(15)). The main signals in ^{13}C NMR (DMSO-d_6): δ (ppm) = 168.78 C8─S,

Table 2
Crystal data, structure solution methods and refinement results for $[Sn(L2)Cl_3]$ (**3**) and $[H_2L2]_2[Ph_2SnCl_4]$ (**4**) complexes

Compound	$[Sn(L2)Cl_3]$	$[H_2L2]_2[Ph_2SnCl_4]$
Empirical formula	$C_{14}H_{13}N_4Cl_3SSn$	$C_{40}H_{40}N_8Cl_4S_2Sn$
Formula weight	494.38	957.41
Temperature (K)	294(2)	293(2)
Crystal system	Monoclinic	Triclinic
Space group	$P2_1/c$	$P\bar{1}$
Unit cell dimensions[a]		
a (Å)	8.353(1)	8.182(1)
b (Å)	13.380(1)	9.179(1)
c (Å)	17.410(1)	15.129(1)
α (°)	90.00	74.925 (2)
β (°)	102.21(1)	81.424(2)
γ (°)	90.00	73.201(2)
Volume (Å^3)	1901.8(3)	1046.94(5)
Z, density calc. (Mg m^{-3})	4, 1.727	1, 1.519
Absorption coefficient, μ (mm^{-1})	1.877	1.006
$F(000)$	968	486
Crystal size (mm)	$0.15 \times 0.11 \times 0.10$	$0.04 \times 0.12 \times 0.16$
Crystal color, shape	Yellow, prism	Yellow, fragment
Diffractometer, scan	KappaCCD/φ and ω	
Rad., graph. Monoch.	Mo Kα, $\lambda = 0.71073$ Å	
θ Range for data coll. (°)	2.84–25.0	3.03–25.00
Index range, θ	$-9 \leqslant h \leqslant 9$	$-9 \leqslant h \leqslant 9$
	$-15 \leqslant k \leqslant 15$	$-10 \leqslant k \leqslant 10$
	$-20 \leqslant l \leqslant 17$	$-17 \leqslant l \leqslant 17$
Completeness	99.7% to $\theta = 25.00°$	99.7% to $\theta = 25.00°$
Absorption correction	GAUSSIAN [24]	None
Max. and min. transm.	0.835 and 0.766	–
Obs. refls. [$I > 2\sigma(I)$]	2590	3327
Data collection	COLLECT [20]	
Data red. and correct.[b] and struct. solute[c] and refinement[d] programs	DENZO and SCALEPACK [21] SHELXS-97 [22] SHELXL-97 [23]	
Refinement method	Full-matrix least-squares on F^2	
Goodness-of-fit on F^2	1.036	1.052
Reflections collected/unique [R_{int}]	16009/3334 [0.0534]	11566/3677 [0.036]
Data/restraints/parameters	3334/0/210	3677/0/270
R_{obs}, R_{all}	0.0353, 0.0539	0.0285, 0.0336
wR_{2obs}, wR_{2all}	0.0818, 0.0927	0.0689, 0.0727
Larg. peak and hole (e Å^{-3})	0.766 and −0.642	0.265 and −0.719

[a] Least-squares refinement of the angular settings for 16009 reflections in the range $2.84° < \theta < 25.00°$ for **3** and 11566 reflections in the range $3.03° < \theta < 25.00°$ for **4**.
[b] Corrections: Lorentz and polarization for **3** and **4** and numerical absorption for **3**. No absorption correction was applied to **4** as μ times crystal dimension was less than 0.16.
[c] Neutral scattering factors and anomalous dispersion corrections.
[d] Structure solved by direct and Fourier methods. The final molecular model obtained by anisotropic full-matrix least-squares refinement of the non-hydrogen atoms.

144.51 C6, 144.39 C4, 141.67 C2, 141.16 C7=N, 129.22 C9, 128.33 C5, 127.53 C3, 29.13 C15. ^{119}Sn NMR (DMSO): δ (ppm) = −477 (s).

2.3.4. $[H_2L2]_2[Ph_2SnCl_4]$ (**4**)

Yellow solid. M.p.: 235.9–237.3 °C. Anal. Calc. $C_{40}H_{40}N_8Cl_4S_2Sn$ (957.41): C, 50.18; H, 4.21; N, 11.70; Sn, 12.40. Found: C, 50.87; H, 4.21; N, 11.54; Sn, 12.90%. IR (CsI pellets, cm^{-1}): 1597m ν(C=N), 790m ν(C=S), 660s ρ(py), 288m ν(M–C), 304w, 237m ν(M–Cl). The main signals in ^{1}H NMR (DMSO-d_6): δ (ppm), *Z* isomer: 12.83 (1H, s, N(3)H), 8.86 (1H, d, H(6)), 8.72 (1H, q, N(4)H), 8.01 (1H, t, H(4)), 7.66–7.26 (1H, m, H(5)), 7.66–7.26 (1H, m, H(3)), 3.09–3.04 (1H, m, H(15)). The main signals in ^{13}C NMR (DMSO-d_6): δ (ppm), *Z* isomer: 178.08 C8=S, 151.48 C2, 148.85 C6, 142.84 C7=N, 138.16 C4, 136.96 C9, 126.02 C3, 124.84 C5, 31.24 C15. The main signals in ^{1}H NMR (DMSO-d_6): δ (ppm), *E* isomer: 9.19 (1H, q, N(4)H), 8.92 (1H, s, N(3)H), 8.56 (1H, d, H(6)), 8.23 (1H, m, H(4)), 8.30 (1H, d, H(3)), 7.66–7.26 (1H, m, H(5)), 3.09–3.04 (1H, m, H(15)). The main signals in ^{13}C NMR (DMSO-d_6): δ (ppm) *E* isomer: 177.62 C8=S, 154.49 C2, 148.68 C6, 136.46 C4, 133.26 C9, 131.13 C7=N, 123.97 C5, 121.64 C3, 31.41 C15.

2.3.5. $[Sn(L3)PhCl_2]$ (**5**)

Orange solid. M.p.: 254.1–256.3 °C. Anal. Calc. $C_{25}H_{20}N_4Cl_2SSn$ (598.10): C, 50.20; H, 3.37; N, 9.37; Sn,

Table 3
Crystal data, structure solution methods and refinement results for [Sn(L3)$PhCl_2$] (**5**) and [Sn(L3)Ph_2Cl] (**6**) complexes

Compound	[Sn(L3)$PhCl_2$]	[Sn(L3)Ph_2Cl]
Empirical formula	$C_{25}H_{20}N_4Cl_2SSn$	$C_{31}H_{25}N_4ClSSn$
Formula weight	598.10	639.75
Temperature (K)	294(2)	294(2)
Crystal system	Monoclinic	Monoclinic
Space group	$P2_1/c$	$P2_1/n$
Unit cell dimensions[a]		
a (Å)	9.180(1)	13.299(1)
b (Å)	12.680(1)	14.381(1)
c (Å)	21.950(1)	15.352(1)
β (°)	101.58(1)	105.85(1)
Volume (Å^3)	2503.0(3)	2824.5(2)
Z, density calc. (Mg m^{-3})	4, 1.587	4,1.504
Absorption coefficient, μ (mm^{-1})	1.339	1.100
$F(000)$	1192	1288
Crystal size (mm)	$0.12 \times 0.08 \times 0.04$	$0.12 \times 0.12 \times 0.12$
Crystal color, shape	Orange, fragment	Yellow, fragment
Diffractometer, scan	KappaCCD/φ and ω	
Rad., graph. monoch.	Mo Kα. $\lambda = 0.71073$ Å	
θ Range for data coll. (°)	3.23–24.99	3.10–25.0
Index range, θ	$-10 \leqslant h \leqslant 10$	$-14 \leqslant h \leqslant 15$
	$-15 \leqslant k \leqslant 12$	$-15 \leqslant k \leqslant 17$
	$-22 \leqslant l \leqslant 26$	$-18 \leqslant l \leqslant 18$
Completeness	99.5% to $\theta = 24.99°$	99.8% to $\theta = 25.00°$
Absorption correction	Multi-scan [18]	
Max. and min. transm.	0.948 and 0.856	0.879 and 0.879
Obs. refls. [$I > 2\sigma(I)$]	3471	3719
Data collection	COLLECT [20]	
Data red. and correct.[b] and struct. solute[c] and refinement[d] programs	DENZO and SCALEPACK [21] SHELXS-97 [22] SHELXL-97 [23]	
Refinement method	Full-matrix least-squares on F^2	
Goodness-of-fit on F^2	1.088	1.076
Reflections collected/unique [R_{int}]	13659/4378 [0.0372]	16081/4962 [0.0427]
Data/restraints/parameters	4378/0/318	4962/0/368
R_{obs}, R_{all}	0.0360, 0.0508	0.0358, 0.0569
wR_{2obs}, wR_{2all}	0.0912, 0.0999	0.0819, 0.0949
Larg. peak and hole (e Å^{-3})	0.826 and −0.691	0.819 and −0.849

[a] Least-squares refinement of the angular settings for 13659 reflections in the range $3.23° < \theta < 24.99°$ for **5** and 16081 reflections in the range $3.10° < \theta < 25.00°$ for **6**.
[b] Corrections: Lorentz, polarization and empirical absorption.
[c] Neutral scattering factors and anomalous dispersion corrections.
[d] Structure solved by direct and Fourier methods. The final molecular model obtained by anisotropic full-matrix least-squares refinement of the non-hydrogen atoms.

19.85. Found: C, 50.44; H, 3.32; N, 9.39; Sn, 20.01%. IR (CsI pellets, cm^{-1}): 1535m ν(C═N), 738s ν(C─S), 640m ρ(py), 272m ν(M–C), 347m ν(M–N), 329w ν(M–S), 241w ν(M–Npy), 216w ν(M–Cl). The main signals in ^{1}H NMR (DMSO-d_6): δ (ppm) = 10.63 (2H, s, N(4)H), 8.32 (1H, d, H(6)), 7.89 (1H, t, H(4)), 7.66 (1H, dd, H(5)), 7.11 (1H, m, H(3)). The main signals in ^{13}C NMR (DMSO-d_6): δ (ppm) = 167.45 C8─S, 153.42 C2, 144.24 C6, 142.23 C7═N, 133.30 C4, 130.77 C9, 127.82 C3, 127.46 C5; 139.73 C21, 132.82 C22 and C26, 128.26 C23 and C25. ^{119}Sn NMR (DMSO): δ (ppm) = −387.

2.3.6. *[Sn(L3)Ph_2Cl] (**6**)*

Yellow solid. M.p.: 185.1–187.2 °C. Anal. Calc. $C_{31}H_{25}N_4ClSSn$ (639.75): C, 58.20; H, 3.94; N, 8.77; Sn, 18.55. Found: C, 57.42; H, 4.04; N, 8.64; Sn, 19.47%. Molar conductivity (1×10^{-3} mol L^{-1} DMF): 51.60 Ω^{-1} cm^2 mol^{-1}. IR (CsI pellets, cm^{-1}): 1542m ν(C═N), 734m ν(C─S), 639w ρ(py), 279w, 266w ν(M–C), 346w ν(M–N), 339w ν(M–S), 285w ν(M–Npy), 228w ν(M–Cl). The main signals in ^{1}H NMR (DMSO-d_6): δ (ppm) = 10.15 (2H, s, N(4)H), 8.82 (1H, d, H(6)), 7.83 (1H, t, H(4)), 7.49 (1H, dd, H(5)), 7.11 (1H, d, H(3)). The main signals in ^{13}C NMR (DMSO-d_6): δ (ppm) = 167.02 C8─S, 155.19 C2, 147.56 C6, 146.88 C7═N, 139.79 C4, 128.22 C9, 126.42 C3, 126.32 C5; 153.65 C21, 132.81 C22 and C26, 128.27 C23 and C25. $^nJ(^{119}Sn^{13}C)$: 1307.4 Hz $^1J(^{119}Sn^{13}C21)$, 66.2 Hz $^2J(^{119}Sn^{13}C22, C26)$, 111.1 Hz $^3J(^{119}Sn^{13}C23, C25)$. ^{119}Sn NMR (DMSO): δ (ppm) = −344 (s).

3. Results and discussion

3.1. Formation of the tin(IV) complexes

Microanalyses and molar conductivity measurements suggest the formation of the following complexes: $[Sn(L1)Cl_3]$ (**1**), $[Sn(L1)PhCl_2]$ (**2**), $[Sn(L2)Cl_3]$ (**3**), $[Sn(L3)PhCl_2]$ (**5**) and $[Sn(L3)Ph_2Cl]$ (**6**), in which an anionic thiosemicarbazone is attached to the metal centre and the remaining coordination sites are occupied either by chloride ions or by both chloride ions and phenyl groups.

Microanalyses of **4** are compatible with the presence of $[H_2L2]_2^+[Ph_2SnCl_4]^{2-}$, which was also corroborated by Mössbauer data and crystal structure determinations (see below).

The formation of complexes **1**–**3**, **5** and **6** can be summarized in Scheme 1.

The formation of the $[Ph_2SnCl_4]^{2-}$ dianion as in **4** is not an uncommon process in tin chemistry. In fact, there are a number of papers describing complexes where such ion is present [9].

3.2. Spectroscopic characterization

The vibrations attributed to ν(C=N) at 1585–1595 cm^{-1} in the infrared spectra of the free thiosemicarbazones shift to 1535–1554 cm^{-1} in the spectra of complexes **1**–**3**, **5** and **6**, in agreement with coordination of the azomethine nitrogen [10]. The ν(C=S) absorption which lays at 796–800 cm^{-1} in the spectra of the ligands shift to 715–738 cm^{-1} in the spectra of complexes **1**–**3**, **5** and **6**, indicating coordination of a thiolate sulfur. The in-plane deformation mode of the pyridine ring at 595–607 cm^{-1} in the spectra of the thiosemicarbazones shift to 633–657 cm^{-1} in complexes **1**–**3**, **5** and **6** suggesting coordination of the hetero-aromatic nitrogen [5,10]. In the spectra of the complexes absorptions at 265–279 cm^{-1} were assigned to ν(Sn–C), those at 346–360 cm^{-1} to ν(Sn–N(imine)), and the bands at 319–339 cm^{-1}, 241–285 cm^{-1} and at 210–308 cm^{-1} to ν(Sn–S), ν(Sn–Npy) and ν(Sn–Cl), respectively [5,11].

The infrared spectrum of H2Bz4Me presents a sharp band at 3298 cm^{-1} along with a broad absorption in the 3300–3250 cm^{-1} range attributed to ν(N3–H) and

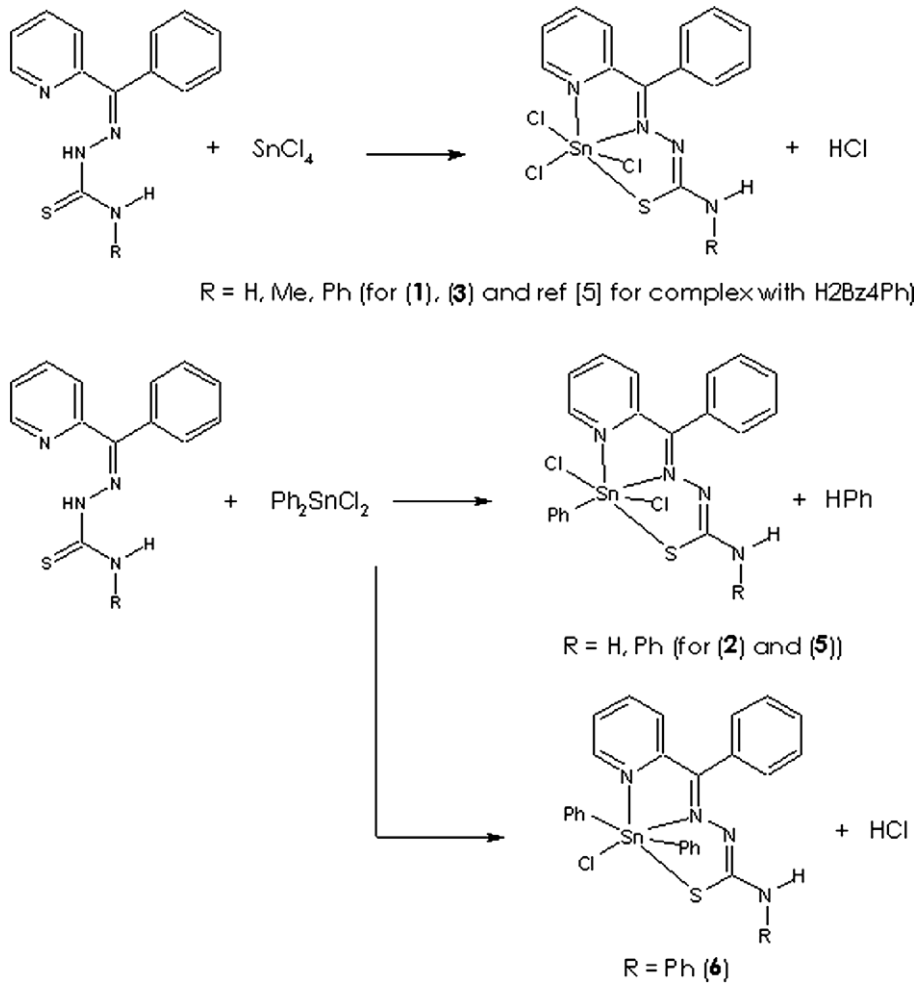

Scheme 1.

ν(N4–H). In the spectrum of **4** a new absorption observed at 3344 cm^{-1} is consistent with protonation at the pyridine nitrogen, which gives rise to an additional N–H stretching vibration. In addition, the in-plane-deformation mode of the pyridine ring at 603 cm^{-1} in the spectrum of the thiosemicarbazone shifts to 660 cm^{-1} in that of **4**.

NMR spectra of **1**–**6** were run in DMSO-d_6 because this is the only solvent in which all ligands and complexes are enough soluble for recording ^{13}C spectra. The ^{1}H resonances were assigned on the basis of chemical shifts, multiplicities and coupling constants. The carbon type (C, CH) was determined by using distortionless enhancement by polarization transfer (DEPT135) experiments. The assignments of the protonated carbons were made by 2D heteronuclear multiple quantum coherence experiments (HMQC) using delay values which correspond to ^{1}J(C, H). A ^{119}Sn NMR study was performed for **1**–**3**, **5** and **6**.

In the ^{1}H and ^{13}C spectra of the uncomplexed thiosemicarbazones all signals are duplicated as a consequence of the existence of structural *Z* and *E* isomers (see Fig. 1) in solution [5,10]. The *Z* form is present in the solids, as shown previously by us [5,10b].

The N3–H signal is absent in the spectra of complexes **1**–**3**, **5** and **6**, in agreement with deprotonation and formation of an anionic ligand. Upon complexation the signals of the pyridine hydrogens undergo significant shifts. Similarly in the ^{13}C NMR spectrum large shifts occur for C=S, C=N and the pyridine carbons, in accordance with coordination of the sulfur, the imine nitrogen and the hetero-aromatic nitrogen, leading to compounds in which the thiosemicarbazone adopts the *E* form which is also adopted in the solids, as revealed by the crystal structures of the complexes (see below).

The ^{1}H and ^{13}C spectra of compound **4** are not appreciably different from those of the free ligand, due probably to exchange of the proton at Npy with deuterium from DMSO-d_6. The ^{1}H and ^{13}C NMR signals are duplicated, indicating that the thiosemicarbazone exists as the *Z* and *E* isomeric forms.

Only one signal was observed in the ^{119}Sn NMR spectra of complexes **1**–**3**, **5** and **6** in agreement with the presence of one tin site. The signals of ^{119}Sn were found at −471 ppm for [Sn(L1)Cl_3] (**1**); −374 ppm for [Sn(L1)$PhCl_2$] (**2**); −477 ppm for [Sn(L2)Cl_3] (**3**); −387 ppm for [Sn(L3)$PhCl_2$] (**5**) and −344 ppm for [Sn(L3)Ph_2Cl] (**6**). The signals of ^{119}Sn in the spectra of **1**–**3**, **5** and **6** recorded in CH_2Cl_2 (data not shown) were found practically at the same positions, indicating that DMSO-d_6 probably did not coordinate to the metal.

Our data suggest that the ^{119}Sn signal shifts to more negative frequencies upon increasing the number of chloride ions in the metal coordination sphere probably due to π back-donation from p-electrons of the halogen to the empty 5d orbitals of tin with appropriate symmetry [12]. Thus, as mentioned above the chemical shifts were −471 ppm for [Sn(2Bz4DH)Cl_3] (**1**) and −374 ppm for [Sn(2Bz4DH)$PhCl_2$] (**2**). Similarly, for [Sn(2Bz4Ph)$PhCl_2$]

Table 4
Selected bond lengths (Å) and angles (°) for [Sn(L1)Cl_3] (**1**), [Sn(L1)$PhCl_2$] (**2**), [Sn(L2)Cl_3] (**3**), [H_2L2]$_2$[Ph_2SnCl_4] (**4**), [Sn(L3)$PhCl_2$] (**5**) and [Sn(L3)Ph_2Cl] (**6**) complexes

Bond	1	2	3	4	5	6	Angle	1	2	3	4	5	6
S1–C8	1.749(4)	1.742(13)	1.757(4)	1.663(3)	1.750(4)	1.749(4)	C8–N3–N2	115.4(3)	115.3(10)	115.2(3)	120.4(2)	116.5(3)	115.4(3)
N1–C2	1.351(5)	1.372(15)	1.362(5)	1.350(3)	1.356(5)	1.343(4)	N4–C8–S	114.7(3)	116.4(9)	114.9(3)	125.5(2)	114.5(3)	114.6(3)
N1–C6	1.342(5)	1.328(16)	1.339(5)	1.328(3)	1.335(5)	1.332(5)	N3–C8–S	129.0(3)	128.3(10)	128.8(3)	118.5(2)	128.3(3)	128.0(3)
N3–C8	1.330(5)	1.333(15)	1.326(5)	1.381(3)	1.311(5)	1.310(4)	N2–Sn–N1	74.32(12)	73.3(3)	74.12(12)	–	71.86(11)	67.62(10)
N4–C8	1.329(6)	1.322(16)	1.332(5)	1.319(3)	1.352(5)	1.357(5)	N1–Sn–Cl1	100.55(9)	81.7(2)	98.01(10)	–	85.29(8)	120.74(7)
Sn–N2	2.198(3)	2.249(8)	2.189(3)	–	2.217(3)	2.322(3)	N2–Sn–Cl1	174.12(9)	83.8(2)	171.70(9)	–	83.46(9)	171.55(8)
Sn–S	2.444(1)	2.492(3)	2.446(1)	–	2.488(1)	2.519(1)	N3–N2–Sn	119.8(2)	122.1(6)	120.8(2)	–	120.9 (2)	122.2 (2)
Sn–N1	2.199(3)	2.253(9)	2.200(3)	–	2.252(3)	2.500(3)	N1–Sn–S	155.13(8)	151.2(3)	154.6(9)	–	150.86(8)	143.40(7)
Sn–Cl1	2.359(2)	2.502(3)	2.352(1)	2.6089(6)	2.470(1)	2.5721(9)	N2–Sn–S	80.84(9)	78.1(2)	80.78(9)	–	79.15(9)	75.78(8)
Sn–Cl2	2.444(2)	2.472(3)	2.416(2)	2.5717(6)	2.512(1)	–	Cl1–Sn–Cl2	91.05(7)	165.15(11)	93.52(7)	89.87(2)	164.93(4)	–
Sn–Cl3	2.428(2)	–	2.451(1)	–	–	–	Cl2–Sn–Cl3	170.33(4)	–	170.16(5)	–	–	–
Sn–C21	–	2.121(11)	–	2.146(2)	2.156(4)	2.134(4)	C21–Sn–C31	–	–	–	–	–	158.02(16)

(**5**) we found −387 ppm and for [Sn(2Bz4Ph)Ph_2Cl] (**6**) we found −344 ppm.

The values of $^1J(^{119}Sn^{13}C)$ have been determined as 296.7 (**2**) and 1307.4 (**6**). The C–Sn–C angle has been calculated for complex **6** based on the Lockhart equation $^1J = 11.4\theta - 875$ [11c]. We found: $\theta = 169°$. Crystal structure determinations (see below) showed that $\theta = 158°$ (**6**), indicating that the structure in solution is not exactly the same as in the solid. The $^nJ(^{119}Sn^{13}C)$ ($n = 2, 3$) coupling constants were determined for complexes **2** and **6**. For **2**, it was also possible to observe the coupling of tin with C(6) in the pyridine ring, $^2J(^{119}Sn^{13}C)$, and we could determine $^4J(^{119}Sn^{13}C24)$ (see Section 2.3.).

The ^{119}Sn NMR spectra of **4** were quite different in DMSO and CH_2Cl_2. In this case reaction with DMSO occurred. Two ^{119}Sn signals have been observed in CH_2Cl_2 at −224 and −378 ppm, which were attributed to the *cis*, *trans* isomers of $[Ph_2SnCl_4]^{2-}$. The existence of these isomers of $[Ph_2SnCl_4]^{2-}$ in the solid was confirmed by the Mössbauer spectrum of **4** (as powder) reported previously by us [13], which showed the presence of two tin sites with parameters compatible with data reported in the literature for *cis*- and *trans* R_2SnX_4 complexes [14,15]. The crystal structure of **4** shows the presence of *trans* $[Ph_2SnCl_4]^{2-}$. Therefore **4** has been fully characterized in the solid by Mössbauer spectroscopy [13] and crystal structure determinations (see below).

3.3. X-ray diffraction analysis

Selected intra-molecular bond distances and angles for complexes **1**–**6** are given in Table 4. H-bond distances and angles for all compounds are detailed in Table 5. Figs. 2–7 are ORTEP [16] drawings of the molecules. Programs and methods used in the X-ray diffraction experiments and structural analysis are detailed in references [17–24].

Crystal and molecular structures of H2Bz4DH [25] and of its N(4)-methyl (H2Bz4Me) and N(4)-phenyl derivatives (H2Bz4Ph) [5,10b] show that in the solid the compounds adopt the *ZZ* configuration in relation to C7–N2 and N3–C8, with an intra-molecular N3–H···N_{py}hydrogen bond.

In **4**, the hetero-aromatic nitrogen is protonated precluding the existence of the N3–H···N_{py} hydrogen bond observed in the structure of H2Bz4Me. The thiosemicarbazone acts as a positively charged $[H_2$2Bz4Me$]^+$, counter-ion of a $[Ph_2SnCl_4]^{2-}$ centrosymmetric octahedral complex. The tin(IV) ion is equatorially coordinated to four chloride ions [Sn–Cl distances of 2.5717(6) and 2.6089(6) Å] and axially to two negatively charged phenyl groups [d(Sn–C) = 2.146(2) Å]. The phenyl ring plane bisects adjacent Sn–Cl bonds.

It is also to be noted, by comparing the molecular configuration of the uncoordinated $[H_2$2Bz4Me$]^+$ ion in **4** (see Fig. 5) with the related anionic ligand in **3** (see Fig. 4), the key role played by the rotational degree of freedom around the N3–C8 bond in the chelating ability of the ligand to form the tin–sulfur bond.

The bond distances in the cationic thiosemicarbazone are different from those in the neutral compound reported previously [10b]. Hence in H2Bz4Me d(N1–C6) = 1.334(2) Å and d(N1–C2) = 1.347(2) Å whereas d(N1–C6) = 1.328(3) Å and d(N1–C2) = 1.350(3) Å in **4**. Other bond distances in the neutral thiosemicarbazone also undergo variations in **4**. Significant differences were found in the C6–N1–C2 [118.1(2)°] and C2–C7–N2, [127.5(1)°] angles in H2Bz4Me, which change to 123.5(2)° and 115.0(2)°, respectively in **4**. The C6–N1–C2 angle is larger in the neutral thiosemicarbazone due to the spatial requirements of the electron pair on the nitrogen, hence confirming that protonation at N_{py} occurs in **4**.

The crystal of complex **4** is further stabilized by intermolecular N1–H1···Cl1 [d(H1···Cl1) = 2.441 Å, ∠(N1–H1···Cl1) = 154.74° and N4–H4···Cl1 (d(H4···Cl1) = 2.511 Å, ∠(N4–H4···Cl1) = 146.91°) hydrogen bonds.

In all other complexes the metal centre is in a quite similar arrangement with the thiosemicarbazone acting as a negatively charged ligand which results from deprotonation at N(3). The bonding closely resembles coordination of these ligands to palladium(II) in previously studied compounds [10a]. The metal is located in a distorted octahedral environment. The ligand defines an equatorial plane of coordination and acts as a tridentate N_{py}–N–S chelating system [Sn–N_{py} bond distances of 2.199(3) (**1**), 2.253(9)

Table 5
Hydrogen bonds distances (Å) and angles (°) for [Sn(L1)Cl_3] (**1**), [Sn(L1)$PhCl_2$] (**2**), [Sn(L2)Cl_3] (**3**), $[H_2L2]_2[Ph_2SnCl_4]$ (**4**), [Sn(L3)$PhCl_2$] (**5**), [Sn(L3)Ph_2Cl] (**6**) with d(H···A) < r(Å) + 2.00 Å and ∠D–H···A > 110°

Compound	D–H···A	d(D–H)	d(H···A)	d(D–H···A)	∠(D–H···A)	A	Symmetry operation
1	N4–H4A–Cl1	0.860	2.488	3.311	160.54	Cl1	[$x - 1/2, -y + 1/2, z - 1/2$]
	N4–H4B–Cl2	0.860	2.470	3.319	169.43	Cl2	[$-x + 1/2, y - 1/2, -z + 3/2$]
2	N4–H4A–Cl1	0.860	2.496	3.308	157.89	Cl1	[$x - 1/2, -y, z + 1/2$]
	N4–H4B–Cl2	0.860	2.699	3.416	141.65	Cl2	[$x - 1, y, z$]
3	N4–H4–Cl3	0.860	2.398	3.258	178.88	Cl3	[$-x + 2, y + 1/2, -z + 1/2$]
4	N1–H1–Cl1	0.860	2.441	3.239	154.74	Cl1	[$-x + 1, -y + 2, -z$]
	N4–H4–Cl1	0.860	2.511	3.265	146.91	Cl1	[$-x + 1, -y + 2, -z$]
5	N4–H4–Cl2	0.860	2.582	3.422	165.91	Cl2	[$-x + 2, y + 1/2, -z + 1/2$]
6	N4–H4–Cl	0.860	2.683	3.494	157.76	Cl	[$-x + 1/2, y - 1/2, -z + 1/2$]

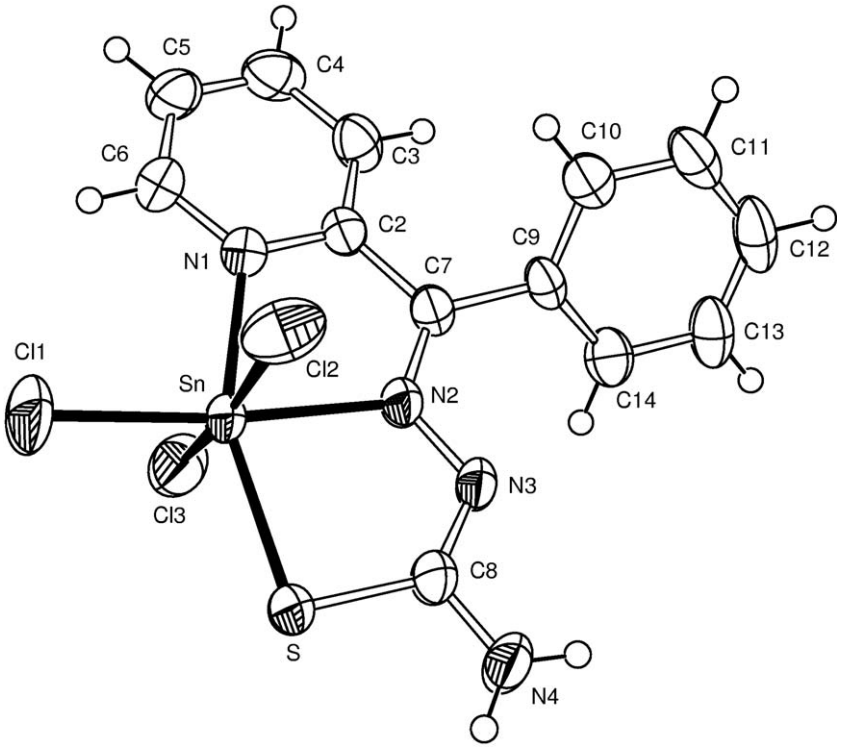

Fig. 2. Molecular plot of $[Sn(L1)Cl_3]$ (**1**) showing the labeling scheme of the non-H atoms and their displacement ellipsoids at the 50% probability level.

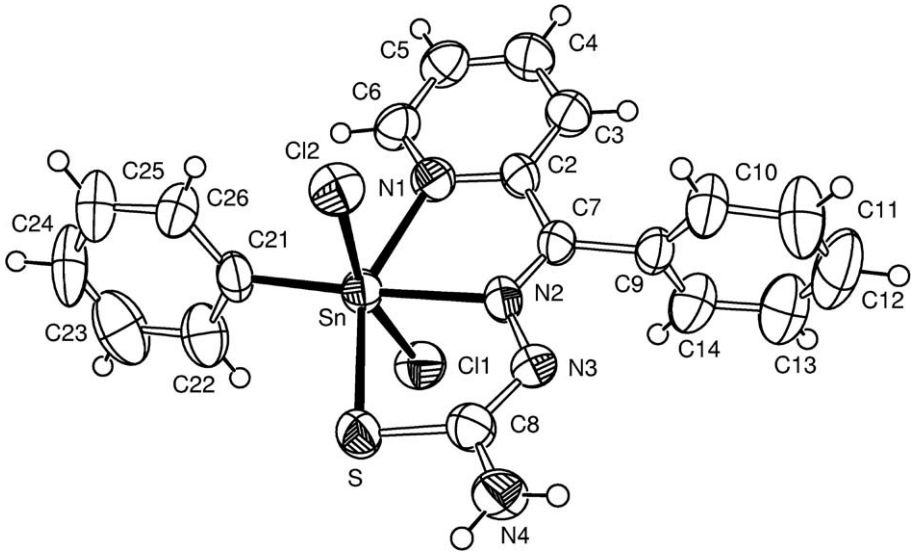

Fig. 3. Molecular structure of $[Sn(L1)PhCl_2]$ (**2**).

(**2**), 2.200(3) (**3**), 2.252(3) (**5**) and 2.500(3) Å (**6**); Sn–N distances of 2.198(3) (**1**), 2.249(8) (**2**), 2.189(3) (**3**), 2.217(3) (**5**), and 2.322(3) Å (**6**), and Sn–S distances of 2.444(1) (**1**), 2.492(3) (**2**), 2.446(1) (**3**), 2.488(1) (**5**), and 2.519(1) Å (**6**)]. The remaining equatorial site is occupied by a negatively charged phenyl ligand in **2** and **5** [d(Sn–C) = 2.12(1) and 2.156(4) Å, respectively] and by a chloride ion in **1**, **3** and **6** [Sn–Cl distances of 2.359(2), 2.352(1), and 2.5721(9) Å, respectively]. The octahedral coordination is completed at the axial positions by two chloride ions in **1** [Sn–Cl distances of 2.444(2) and 2.428(2) Å], **2** [Sn–Cl distances of 2.502(3) and 2.472(3) Å], **3** [Sn–Cl distances of 2.352(1) and 2.416(2) Å], and **5** [Sn–Cl distances of 2.470(1), and 2.512(1) Å, respectively], and by two phenyl anions in **6** [Sn–C distances of 2.132(4) and 2.134(4) Å].

The expected lengthening of the C8═S bond [from 1.663(2)–1.680(2) Å in the ligands to 1.742(13)–1.757(4) Å in **1**–**3**, **5** and **6**] and shortening of the N3–C8 bond [from 1.360(2)–1.367(2) Å in the ligands to 1.310(4)–1.333(15) Å in **1**–**3**, **5** and **6**] upon coordination is observed. Therefore

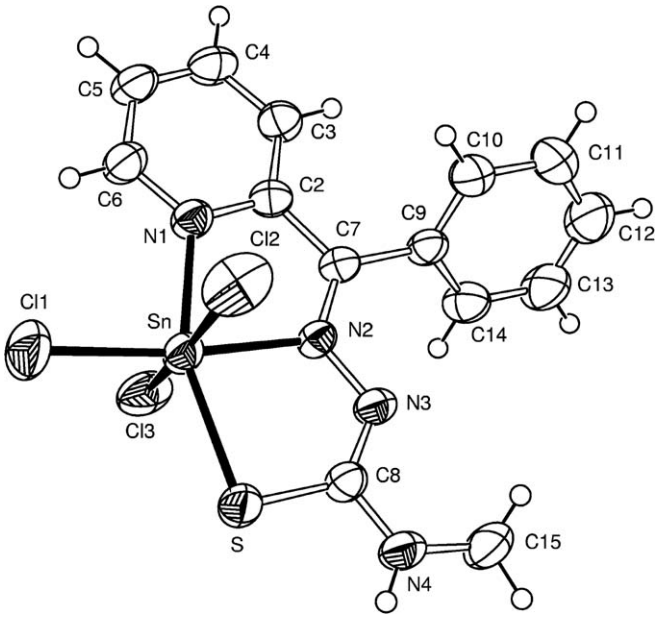

Fig. 4. Molecular structure of $[Sn(L2)Cl_3]$ (**3**).

the C–S bond changes from a double to a predominantly single bond whereas N3–C8 acquires some double bond character.

Furthermore, in the tin complexes the Pyr(C═N)N$^-$(C═S)N skeletal fragment of the ligand molecules are nearly planar [rms deviation of atoms from least-squares plane of 0.0924 Å (**1**), 0.048 Å (**2**), 0.045 Å (**3**), 0.087 Å (**5**), and 0.058 Å (**6**)] with the tin metal laying close onto the coordination plane (at less than 0.17 Å).

As already mentioned, a twisting of 180° in the N2–N3 bond of thiosemicarbazones to match the steric requirements of tridentate coordination was evidenced. Hence some dihedral angles in the free ligands undergo significant changes on complexation. The C8–N3–N2 angle goes from 117.1(1)° in free H2Bz4DH [25] to 115.4(3)° in **1** and 115.3(10)° in **2**; N3–C8–S goes from 119.4(1)° in the free ligand [25] to 129.0(3)° in **1** and 128.3(10)° in **2**; N4–C8–S varies from 124.7(1)° in the ligand [25] to 114.7(3)° in **1** and 116.4(9)° in **2**.

Similarly in free H2Bz4Me ∠(C8–N3–N2) = 119.3(2)°, ∠(N3–C8–S) = 118.3(2)° and ∠(N4–C8–S) = 124.8(2)° [10b]. These angles change to 115.2(3)°, 128.8(3)° and 114.9(3)°, respectively, in complex **3**. In H2Bz4Ph the C8–N3–N2 angle is 120.5(2)°; N3–C8–S is 117.7(1)° and N4–C8–S, 128.0(1)° [5] and upon coordination they change to 116.5(3)°, 128.3(3)° and 114.5(3)°, respectively, in complex **5** and to 115.4(3)°, 128.0(3)° and 114.6(3)°, respectively, in **6**. In **6** the C31–Sn–C21 angle is 158.0(2)° which differs considerably from that corresponding to perfect octahedral geometry.

In complex **1** inter-molecular N4–H4A···Cl1 [*d*(H4A···Cl1) = 2.488 Å, ∠(N4–H4A···Cl1) = 160.54°] and N4–H4B···Cl2 [*d*(H4B···Cl2) = 2.470 Å, ∠(N4–H4B···Cl2) = 169.43°] bonds were observed. Similarly, in **2** N4–H4A···Cl1 [*d*(H4A···Cl1) = 2.496 Å, ∠(N4–H4A···Cl1) = 157.89°] and N4–H4B···Cl2 [*d*(H4B···Cl2) = 2.699 Å, ∠(N4–H4A···Cl2) = 141.65°] bonds were evidenced, in which the chlorides are located in a second molecule. In complexes **3**, **5** and **6** intermolecular N4–H4···Cl bonds were also observed [*d*(H4A···Cl) = 2.398 Å, ∠(N4–H4A···Cl) = 178.88° for **3**; *d*(H4A···Cl2) = 2.582 Å, ∠(N4–H4A···Cl2)

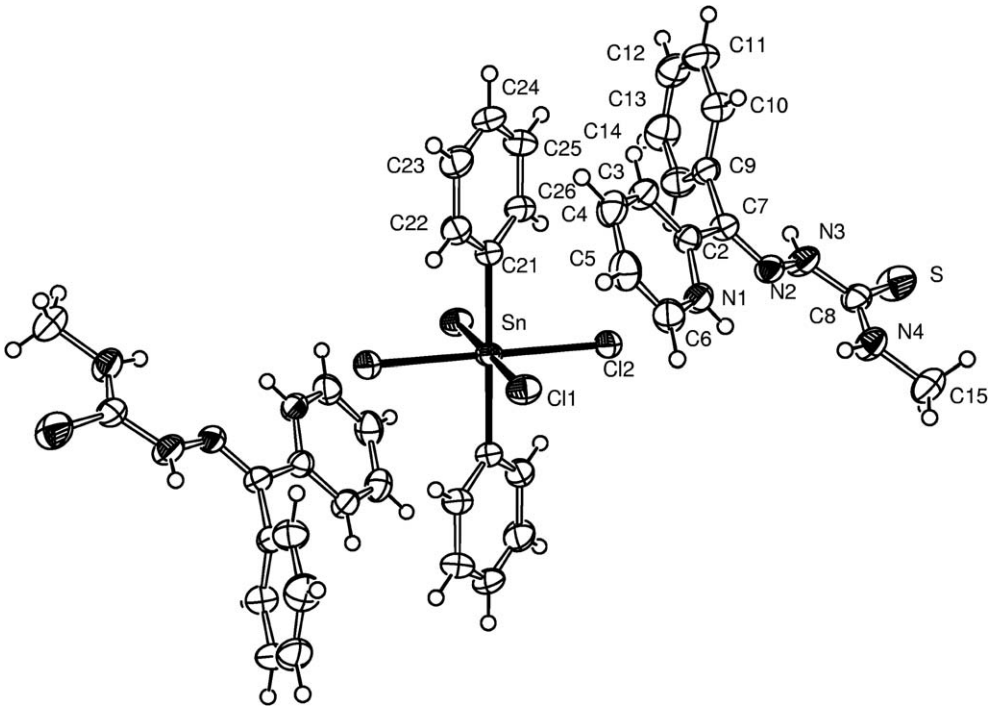

Fig. 5. View of centro symmetric $[H_2L2]_2[Ph_2SnCl_4]$ (**4**).

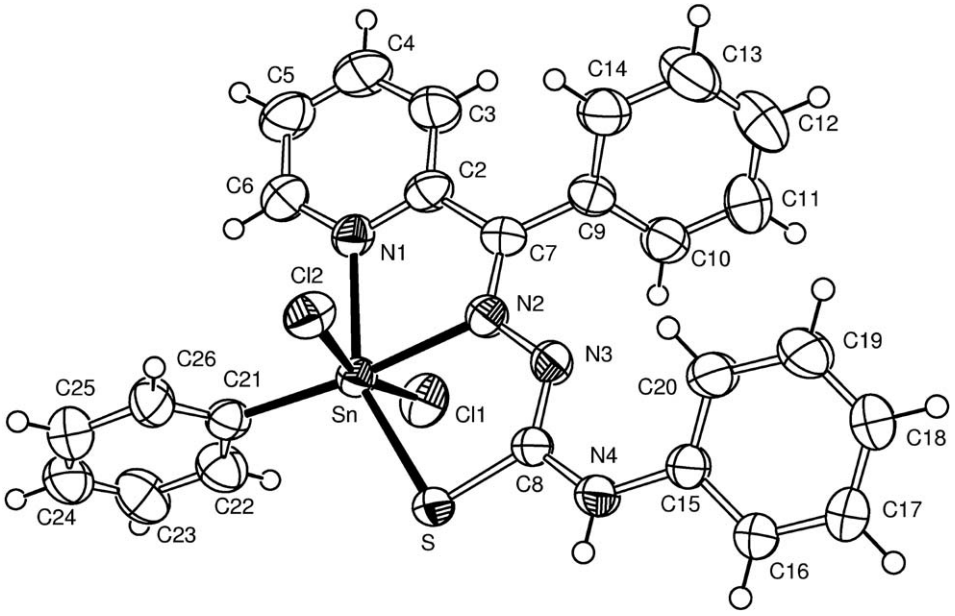

Fig. 6. Molecular structure of $[Sn(L3)PhCl_2]$ (**5**).

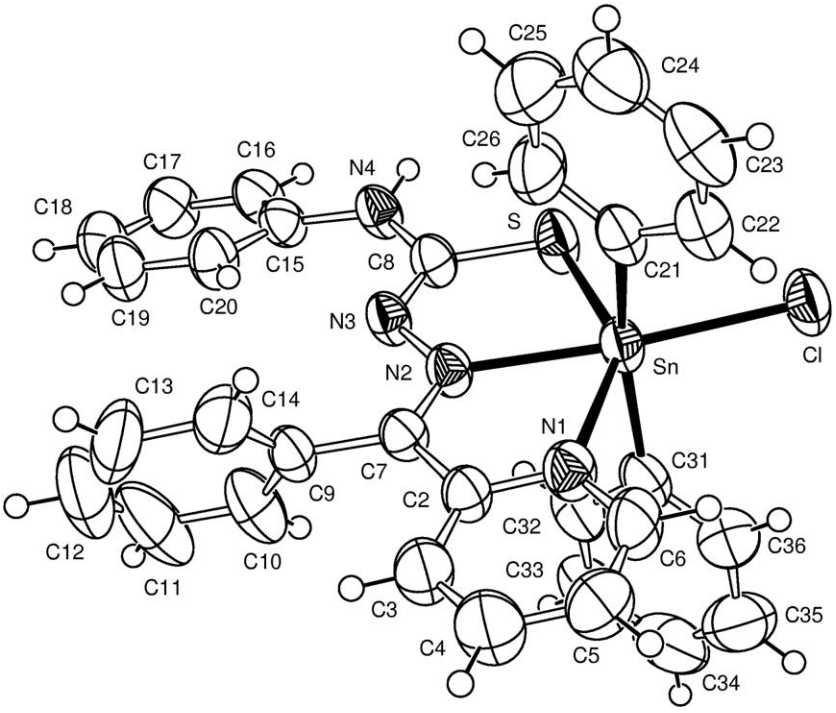

Fig. 7. Molecular structure of $[Sn(L3)Ph_2Cl]$ (**6**).

$= 165.91°$ for **5**, and $d(H4A\cdots Cl) = 2.683$ Å, $\angle(N4–H4A\cdots Cl) = 157.76°$ for **6**] (see Table 5).

4. Supplementary material

Crystallographic data for complexes **1**–**6** have been deposited with the Cambridge Crystallographic Data Center, CCDC numbers 297869 (**1**), 297870 (**2**), 297871 (**3**), 297872 (**4**), 297873 (**5**), 297874 (**6**). Copies of this information may be obtained free of charge from: The Director, CCDC, 12, Union Road Cambridge, CB2 1EZ, UK, fax: +44 1223 336 033; e-mail: deposit@ccdc.cam.ac.uk or via www.ccdc.cam.ac.uk/data_request/cif.

Acknowledgements

This work was supported by Capes and CNPq of Brazil and by CONICET of Argentina.

References

[1] H. Beraldo, D. Gambino, Mini. Rev. Med. Chem. 4 (2004) 31.

[2] (a) D. Kovala-Demertzi, P. Tairidou, U. Russo, M. Gielen, Inorg. Chim. Acta. 239 (1995) 177;
(b) M. Kemmer, M. Gielen, M. Biesemans, D. de Vos, R. Willem, Metal-Based Drugs 5 (1998) 189;
(c) M. Gielen, H. Dalil, B. Mahieu, D. de Vos, M. Biesemans, R. Willem, Metal-Based Drugs 5 (1998) 275;
(d) M. Gielen, Appl. Organometal. Chem. 16 (2002) 481, and references therein;
(e) M. Gielen, M. Biesemans, R. Willem, Appl. Organometal. Chem. 19 (2005) 440, and references therein;
(f) M. Gielen, J. Braz. Chem. Soc. 14 (2003) 870, and references therein.

[3] J.S. Casas, M.S. García-Tasende, C. Maichle-Mössmer, M.C. Rodriguez-Argüelles, A. Sanchez, J. Sordo, A. Vasquez-Lopez, S. Pinelli, P. Lunghi, R. Albertini, J. Inorg. Biochem. 62 (1996) 41.

[4] J.S. Casas Casas, M.C. Rodriguez-Argüelles, U. Russo, A. Sanchez, J. Sordo, A. Vasquez-Lopez, S. Pinelli, P. Lunghi, A. Bonati, R. Albertini, J. Inorg. Biochem. 69 (1998) 283, and references therein.

[5] A.P. Rebolledo, G.M. de Lima, L.N. Gambi, N.L. Speziali, D.F. Maia, C.B. Pinheiro, J.D. Ardisson, M.E. Cortés, H. Beraldo, Appl. Organometal. Chem. 17 (2003) 945.

[6] A. Pérez-Rebolledo, J.D. Ayala, G.M. de Lima, N. Marchini, G. Bombieri, C.L. Zani, E.M. Souza-Fagundes, H. Beraldo, Eur. J. Med. Chem. 40 (2005) 467.

[7] D.X. West, I.S. Billeh, J.P. Jasinski, J.M. Jasinski, R.J. Butcher, Transit. Met. Chem. 23 (1998) 209.

[8] D.X. West, J.S. Ives, J. Krejci, M. Salberg, T.L. Zumbahlen, G. Bain, A. Liberta, J.V. Martinez, S.H. Ortiz, R. Toscano, Polyhedron 14 (1995) 2189.

[9] (a) R. Venkatraman, P.C. Ray, F.R. Fronczek, Acta Crystallogr., Sect. E 60 (2004) m1035, and references therein;
(b) J.S. Casas, A. Castiñeiras, M.D. Couce, G. Martinez, J. Sordo, J.M. Varela, J. Organomet. Chem. 517 (1996) 165;
(c) J.F. Vollano, R.O. Day, R.R. Holmes, Organometallics 3 (1984) 745.

[10] (a) A.P. Rebolledo, M. Vieites, D. Gambino, O.E. Piro, E.E. Castellano, C.L. Zani, E.M. Souza-Fagundes, L.R. Teixeira, A.A. Batista, H. Beraldo, J. Inorg. Biochem. 99 (2005) 698;
(b) R.F.F. Costa, A.P. Rebolledo, T. Matencio, H.D.R. Callado, J.D. Ardisson, M.E. Cortés, B.L. Rodrigues, H. Beraldo, J. Coord. Chem. 58 (2005) 1307.

[11] (a) A.K. Nakamoto, Infrared and Raman Spectra of Inorganic and Coordination Compounds, fourth ed., John Wiley & Sons, Inc., New York, 1986;
(b) C. Pettinari, M. Pellei, C. Santini, I. Natali, F. Accorroni, A. Lorenzotti, Polyhedron 17 (1998) 4487;
(c) F. Caruso, M. Giomini, A.M. Guiliani, E.J. Rivarola, J. Organometal. Chem. 466 (1994) 69.

[12] R.K. Harris, J.D. Kennedy, W. McFarlane, in: R.K. Harris, B.E. Mann (Eds.), NMR and the Periodic Table, Academic Press, London, 1978, p. 342.

[13] A. Pérez-Rebolledo, J.D. Ardisson, G.M. de Lima, W.A.A. Macedo, H. Beraldo, Hyperfine Interact. 163 (2005) 1.

[14] B.W. Fitzsimmons, N.J. Seeley, A.W. Smith, J. Chem. Soc. (A) (1969) 143.

[15] J.L. Wardell, G.M. Spencer, Tin: organometallic chemistry, in: Encyclopedia of Inorganic Chemistry, Wiley. (Org.), New York, 1994, p. 4172.

[16] C.K. Johnson, ORTEPII. Report ORNL-5138, Oak Ridge National Laboratory, Tennessee, USA, 1976.

[17] C.W. Dwiggins Jr., Acta Crystallogr., Sect. A 31 (1975) 146.

[18] R.H. Blessing, Acta Crystallogr., Sect. A 51 (1995) 33.

[19] Siemens XSCANS Users Manual, Siemens Analytical X-ray Instruments, Madison, WI, 1994.

[20] Enraf-Nonius COLLECT. Nonius BV, Delft, The Netherlands, 1997–2000.

[21] Z. Otwinowski, W. Minor, in: C.W. Carter, R.M. Sweet (Eds.), Methods in Enzymology, vol. 276, Academic Press, New York, 1997, p. 307.

[22] G.M. Sheldrick, SHELXS-97, Program for the Solution of Crystal Structures, University of Göttingen, Göttingen, Germany, 1997.

[23] G.M. Sheldrick, SHELXL-97, Program for Crystal Structures Analysis, University of Göttingen, Göttingen, Germany, 1997.

[24] P. Coppens, L. Leiserowitz, D. Rabinovich, Acta Crystallogr. 18 (1965) 1035.

[25] J.S. Casas, E.E. Castellano, J. Ellena, M.S. García Tasende, A. Sánchez, J. Sordo, M.J. Vidarte, Inorg. Chem. 42 (2003) 2584.